Biochemical Pharmacology 78 (2009) 1178–1185

Contents lists available at ScienceDirect

Biochemical Pharmacology

journal homepage: www.elsevier.com/locate/biochempharm

Inhibitory mechanisms of heterocyclic carboxaldehyde thiosemicabazones for two forms of human ribonucleotide reductase☆

Lijun Zhu [a], Bingsen Zhou [b], Xinhuan Chen [a], Hongjuan Jiang [a], Jimin Shao [a,*], Yun Yen [b,**]

[a] Department of Pathology and Pathophysiology, Zhejiang University School of Medicine, Hangzhou, Zhejiang 310058, PR China
[b] Division of Clinical and Molecular Pharmacology, City of Hope National Medical Center, 1500 East Duarte Road, Duarte, CA 91010, USA

ARTICLE INFO

Article history:
Received 12 May 2009
Accepted 24 June 2009

Keywords:
Ribonucleotide reductase
The small subunits M2 and p53R2
Heterocyclic carboxaldehyde thiosemicarbazones (HCTs)
3-Aminopyridine-2-carboxaldehyde thiosemicarbazone (3AP)
Mechanism of action

ABSTRACT

Two forms of ribonucleotide reductase (RR), consisting of M1 with M2 subunits and M1 with p53R2 subunits, are involved in DNA replication and damage repair, respectively. 3-Aminopyridine-2-carboxaldehyde thiosemicarbazone (3AP), one of the heterocyclic carboxaldehyde thiosemicabazones (HCTs), is a potent RR inhibitor in clinical trial for cancer treatment. In this study, 3AP and its 7 derivatives showed 100–1000-fold higher inhibitory potency on KB nasopharyngeal carcinoma cells than hydroxyurea and were fully active against hydroxyurea- and gemcitabine-resistant KB cells. In vitro RR assays using two recombinant RRs showed that all 8 HCTs decreased the activity of both RRs in a dose-dependent manner and the efficiency was compatible with that on cell proliferation inhibition. Iron has different impact on the behavior of the compounds toward RRs. In the absence of iron, the HCTs showed more selective inhibition for p53R2–M1 than M2–M1, while addition of iron increased their activity but reduced their selectivity for two RRs. Radioligand binding assays showed that [^{3}H]3AP directly bounded to the small subunits. Electron paramagnetic resonance measurements demonstrated that these HCTs generated reactive oxygen species with ferrous iron, which quenched the diiron-tyrosyl radical co-factor of the small subunits and hence the enzyme activity. While the ROS may be a common mediator responsible for the potent activity of the HCTs, the different characteristics of the small subunit proteins are probably associated with the subunit-selectivity of inhibition. Better understanding of the mechanism of action of RR inhibition may improve design of new potent and subunit-selective RR inhibitors for cancer therapy.

1. Introduction

Ribonucleotide reductase (RR) catalyzes the reduction of ribonucleotides to their corresponding deoxyribonucleotides, which are the building blocks for DNA synthesis [1]. Human RR consists of two dimers: M1 (large subunit) and M2 or p53R2 (small subunit), constituting two forms of RR in human cells (M2–M1 and p53R2–M1) [2,3]. M1 contains the active site and binding sites for allosteric effectors. M2 and p53R2 are homologue (~80%), both possess a diiron-tyrosyl radical co-factor that is essential for enzyme activity. The conserved functional domains between the two small subunits include the iron ligands, the radical site tyrosine, the radical transfer pathway from the small subunit to the large subunit, and the C-terminal sequence for binding to the large subunit. The major sequence difference between the two small subunits is that p53R2 lacks 33 amino acid residues in its N-terminus [4,5]. The reaction rate of p53R2 was lower than that of M2, which may be due to its reduced binding affinity to M1 [6]. M2–M1 and p53R2–M1 function in DNA replication and repair, respectively. M2 is cell cycle-regulated via S-phase-specific transcription and proteasome-mediated degradation in late mitosis. The expression of p53R2 is induced by DNA damaging agents in a p53-dependent manner [2,3]. p53 also directly interacts with p53R2 to promote its translocation to the nucleus to supply deoxynucleotides for DNA repair [7]. ATM-dependent p53R2 Ser72 phosphorylation stabilizes p53R2 protein by inhibiting p53R2 hyperubiquitination and degradation by MDM2 in response to DNA damage [8]. These findings lead to the hypothesis that there are two pathways in human cells to supply deoxynucleotides for DNA synthesis: one through the activity of M2, involved in normal maintenance of deoxynucleotides for DNA replication during the S/G2 phases in a cell cycle-dependent manner, and the other through p53R2, supplying deoxynucleotides for DNA repair in

☆ This project has been partially supported by Phase I foundation grant.
Abbreviations: RR, ribonucleotide reductase; KB-WT, human KB nasopharyngeal carcinoma wild-type cells; KB-HU, KB hydroxyurea-resistant cells; KB-GEM, KB gemcitabine-resistant cells; EPR, electron paramagnetic resonance; 3AP, 3-aminopyridine-2-carboxaldehyde thiosemicarbazone; HCTs, heterocyclic carboxaldehyde thiosemicabazones; HU, hydroxyurea; GEM, gemcitabine.
* Corresponding author. Tel.: +86 571 88208209; fax: +86 571 88208209.
** Corresponding author. Tel.: +1 626 256 4673x65707; fax: +1 626 471 7204.
E-mail addresses: shaojimin@zju.edu.cn (J. Shao), yyen@coh.org (Y. Yen).

0006-2952/$ – see front matter © 2009 Elsevier Inc. All rights reserved.
doi:10.1016/j.bcp.2009.06.103

G_0/G_1 cells in a p53-dependent manner [9–11]. Recent findings suggest that p53R2 also plays an essential role in supplying deoxynucleotides for basal repair of DNA and mtDNA synthesis in G_0/G_1 cells [12–14].

Increased RR activity, especially over-expression of M2, has been associated with malignant transformation and cancer metastasis [15–17]. Tumor cells are more sensitive to the cytotoxic effect of RR inhibition than normal cells because of the increased need of deoxynucleotides for proliferation. Inactivation of RR stops DNA synthesis, which inhibits cell proliferation, making it an important target for anticancer agents. The discovery of p53R2 raises high interests in the role of p53R2 in the development of human cancers [2,4,9,10]. In oral and esophageal squamous cell carcinoma and colon adenocarcinoma, p53R2 expression was related to tumor growth, invasion, and metastasis [18–20]. Common inhibitors for both forms of RR may be important for complete inactivation of RR in cells, while specific inhibitors for each small subunit may exhibit different clinical values because M2 and p53R2 play different roles in cells [9,21,22].

The inhibitors of RR can be divided into different categories. The large subuint inhibitors can inhibit the active site or induce allosteric malfunction by nucleoside analogs, such as gemcitabine (GEM) [23]. The small subunit inhibitors destroy the essential diiron-tyrosyl radical center using radical scavengers or iron chelators, such as hydroxyurea (HU) and triapine (3-aminopyridine-2-carboxaldehyde thiosemicarbazone, 3-AP) [24,25]. Polymerization inhibitors interfere with RR holoenzyme assembly by oligopeptides corresponding to the c-terminus of the small subunits [26]. Heterocyclic carboxaldehyde thiosemicabazones (HCTs) are a class of powerful iron chelators, which coordinate with iron through the N*–N*–S* tridentate ligand system to form a 2:1 ligand to iron molar ratio octahedral complex [27]. 3-AP, one of the HCTs, is a new RR inhibitor currently being tested in clinical trials for cancer therapy [25,28]. This compound is more potent inhibitor of RR and tumor cell growth than HU, and increases the effectiveness of other DNA damaging and cytotoxic agents. It targets the diiron-tyrosyl radical center of the small subunits and the ferrous complex of 3AP is a much more potent inhibitor of RR than 3AP alone and its ferric complex [29,30]. HU has been used in human cancer treatment for decades and is known to specifically inhibit the small subunits by reducing the tyrosyl radical and the iron center [24]. Several schiff bases of hydroxysemicarbazide that are derivatives of HU, has been investigated for their inhibitory potency and selectivity for two forms of RR [31].

In this study, the molecular mechanisms of action of 8 HCTs including 3AP were further examined. It is demonstrated that these HCTs possess much higher potency in both enzyme and tumor cell growth inhibition than HU, and fully active against HU- and GEM-resistant tumor cells. Directly binding to the small subunits and quenching the diiron-tyrosyl radical center via generating reactive oxygen species with ferrous iron are the common property of these HCTs for inactivation of the two forms of RR. The characteristics of the iron chelators and the small subunit proteins are associated with the potency and subunit-selectivity of these compounds. These findings may provide a new basis for the discovery of new potent and subunit-selective RR inhibitors and for improvement of clinical application of the small subunit inhibitors for cancer therapy.

2. Materials and methods

2.1. Chemicals

3AP was a gift from Vion Pharmaceuticals, Inc. (New Haven, CT). 5-Aminopyridine-2-carboxaldehyde thiosemicarbazone (5AP), 3-amino-4-methylpyridine-2-carboxaldehyde thiosemicarbazone (3AMP), 3-methyl aminopyridine-2-carboxaldehyde thiosemicarbazone (3MAP), 3,5-diaminopyridine-2-carboxaldehyde thiosemicarbazone (DAP), 5-amino-4-morpholinomethylpyridine-2-carboxaldehyde thiosemicarbazone (5AMoP), 5-methyl-4-amino-1-formylisoquinoline thiosemicarbazone (MAIQ), and 5-hydroxy-4-methyl-1-formylisoquinoline thiosemicarbazone (HMIQ) (Fig. 1) were kindly provided by Dr. Alan C. Sartorelli (Department of Pharmacology, Yale University School of Medicine). All these HCTs were dissolved in neat DMSO (Sigma, St. Louis, MO) and diluted with 50 mM Tris–HCl buffer (pH 7.2). Hydroxyurea (Sigma) and Gemcitabine (Eli Lilly, Indianapolis, IN) were used as purchased. 5,5-Dimethyl-1-pyrroline-N-oxide (DMPO) was supplied by Sigma.

2.2. Cell proliferation inhibition assay and real-time cell electronic sensing

Human oropharyngeal carcinoma KB cells (KB-WT) from the American Type Culture Collection (Manassas, VA) were cultured in RPMI 1640 supplemented with 10% (v/v) fetal bovine serum in a 5% CO_2 humidified atmosphere at 37 °C. KB hydroxyurea-resistant cells (KB-HU) were selected in a stepwise manner in the presence of HU, cloned, and maintained under a selection pressure of 1 mM HU [32]. A Gemcitabine-resistant clone (KB-GEM) was selected

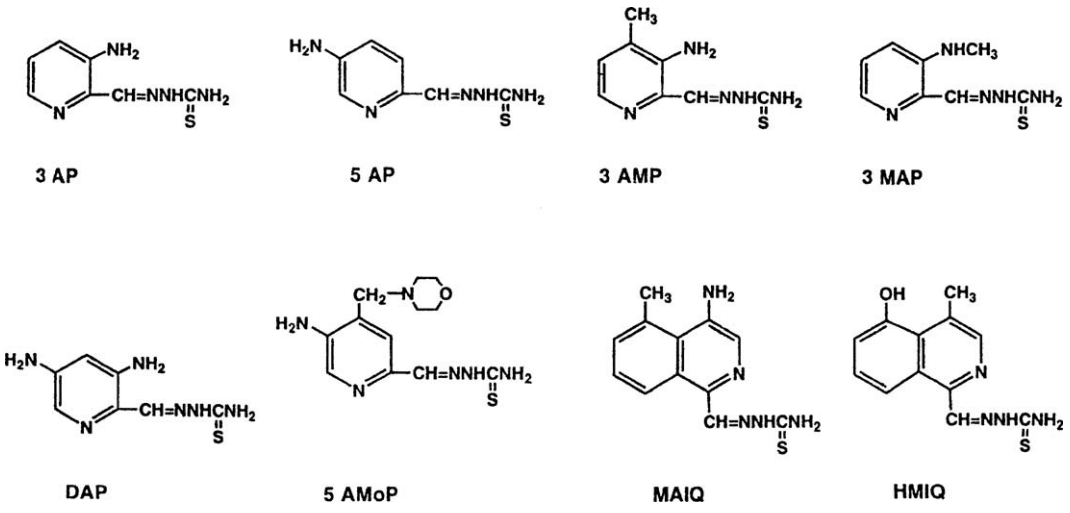

Fig. 1. Structures of heterocyclic carboxaldehyde thiosemicabazones.

with a similar way and maintained in the presence of 8 μM GEM [33]. The resistant cells were grown in drug-free medium for 48 h prior to use. Cells in logarithmic growth were seeded at a density of 50,000 cells/ml in 24-well plates. After 24 h, solutions of HU, GEM, and each of the HCTs were added to cells for cytotoxicity determination. Cultures were incubated for 72 h and subsequently methylene blue assays were performed. The IC50 values (50% cell growth inhibition) were determined using seven different concentrations of each compound. The concentration of DMSO in the cell cultures was 1% (v/v) for the initial (highest) compound concentration and the corresponding control.

The dynamic inhibitory effect of each compound on cell growth was investigated by a real-time cell electronic sensing assay [34]. KB-WT cells were plated at a density of 20,000 cells/ml into wells of 96-well devices compatible with a real-time cell electronic sensing system (RT-CES) (ACEA Biosciences, San Diego, CA). After incubation for 48 h, different concentrations of each compound were added to test wells and further incubated for 72 h. The solvent DMSO was used as a negative control. Cell growth was monitored every 0.5 h for 5-day duration via calculation of a "cell index" (normalized impedance) for each well [35].

2.3. Preparation of recombinant proteins

The coding sequences of M2, p53R2, and M1 were cloned in-frame with a N-terminal 6× His-tag into the prokaryotic expression vector pET28 (Novagen, Madison, WI). The proteins were expressed in BL21 (DE3) bacteria (Stratagene, La Jolla, CA) and purified using Ni(II) affinity chromatography (Qiagen, Valencia, CA) [6]. The purified proteins (in 50 mM Tris–HCl, pH 7.4, 100 mM KCl) were stored at −70 °C. Protein concentration was measured with the Bio-Rad Protein Assay kit (Bio-Rad, Hercules, CA). Protein purity was determined by SDS-PAGE.

2.4. In vitro RR activity assay

The enzymatic activity of recombinant RR was measured using a previously reported [^{3}H] CDP reduction method [31]. Briefly, 100 μl of reaction mixture contained 0.125 μM [^{3}H] CDP (24 Ci/mmol), 50 mM HEPES (pH 7.2), 6 mM DTT, 4 mM MgOAc, 2 mM ATP, 0.05 mM CDP, 100 mM KCl, and 0.25 μM RR holoenzyme (5 μg of M1 and 2.5 μg of M2 or p53R2). The molar amount of holoenzyme was calculated using the MW of the tetramer. Where indicated, up to 60 μM $FeCl_3$ was added to the reaction mixture. After incubation at 37 °C for 30 min and dephosphorylation, samples were analyzed by HPLC and liquid scintillation counting. The specific enzymatic activity was 80.3 ± 2.92 nmol of dCDP/min/mg for M2–M1 and 53.7 ± 2.09 nmol of dCDP/min/mg for p53R2–M1.

For inhibition assays, various concentrations of each compound were incubated with 0.25 μM RR holoenzyme (M2–M1 or p53R2–M1) at room temperature for 30 min followed by the enzymatic activity assay. Negative control samples, which were run with each experiment, contained 1% (v/v) DMSO. The extent of enzyme inhibition was expressed as a percentage of the negative control (relative activity). The IC_{50} values are the compound's concentration that produces 50% inhibition of RR activity.

2.5. Spin trapping experiments and electron paramagnetic resonance (EPR) measurements

Ferrous complexes of the tested HCTs formed readily by mixing each HCT with ferric chloride (2:1 ligand to metal ratio) and DTT at room temperature [30,36]. Solutions for spin trapping experiments contained 1 mM each of the tested HCTs or its ferrous complex, 5% DMSO, and 100 mM DMPO in 50 mM HEPES buffer (pH 7.5). The EPR spectrum of each test solution was measured soon after mixing the reagents. X-band EPR spectra were measured with a Bruker EMX spectrometer at room temperature (~22 °C). For frozen solution EPR measurements, samples of M2 or p53R2 (35 μM) in 50 mM Tris–HCl (pH 7.4) buffer containing 100 mM KCl were incubated at RT for 30 min with 5 μM each of the ferrous complexes of the tested HCTs, separately. The samples were transferred to standard EPR tubes and frozen using liquid nitrogen. Frozen solution EPR spectra were measured using the Bruker EMX spectrometer equipped with an Oxford helium cryostat.

2.6. Radioligand binding assay

Radioligand-protein binding assays were performed using a centrifugal gel filtration method. Sephadex G-50 (fine, Sigma) columns were prepared in tuberculin syringes with 1 ml bed volume of the gel that had been swollen in dH_2O overnight at 4 °C. All centrifugations were for 4 min at 100 × *g* at 10 °C in a centrifuge equipped with a horizontal rotor. The syringe columns were pre-centrifuged and equilibrated with the binding buffer (50 mM Tris–HCl, pH 7.5, 100 mM KCl). [^{3}H]-labelled 3AP (Moravek Biochemicals, Inc., Brea, CA) was incubated with the recombinant RR subunit or holoenzyme proteins in a final volume of 100 μl for 15 min at 37 °C, where indicated $FeCl_3$ and/or DTT was added in the incubation mixture. The incubation mixture was applied to the syringe column and centrifuged. Four aliquots of column filtrates, 100 μl per aliquot, were collected for each sample. Radioactivity in the column filtrates was measured by liquid scintillation counting, and the protein content was determined using the Bio-Rad Protein Assay kit.

3. Results

3.1. The HCTs are much potent than hydroxyurea and fully active against hydroxyurea- and gemcitabine-resistant KB cells

The inhibitory activities of 8 HCTs (Fig. 1), hydroxyurea (HU), and gemcitabine (GEM) against human oropharyngeal carcinoma KB-WT, KB-HU, and KB-GEM cells were determined using cell proliferation assays. The IC50s of 3AP and its 7 HCT analogs were 0.37–7.24 μM for KB-WT, 0.39–2.42 μM for KB-HU, and 0.76–3.98 μM for KB-GEM, respectively (Table 1). The inhibitory potency of these HCTs was about 100–1000-fold higher for KB-WT than that of HU. KB-HU and KB-GEM showed similar sensitivity to these HCTs as KB-WT, indicating no cross-resistance between these HCTs and HU or GEM. Time course of cell growth inhibition was monitored by a real-time cell electronic sensing instrument. Compared to the vehicle, 3AP and HU showed a similar dynamic inhibitory pattern but with about 1000-fold different potency

Table 1
Cytotoxicity of the HCTs.

Compound	IC50 ± S.D. (μM)[a]		
	KB-WT	KB-HU	KB-GEM
3AP	0.693 ± 0.054	0.760 ± 0.069	1.02 ± 0.115
5AP	0.904 ± 0.082	0.897 ± 0.051	3.46 ± 0.221
3AMP	0.762 ± 0.079	0.791 ± 0.066	3.98 ± 0.280
3MAP	0.556 ± 0.055	0.589 ± 0.052	0.758 ± 0.051
DAP	0.370 ± 0.029	0.394 ± 0.029	2.04 ± 0.175
5AMoP	7.24 ± 0.723	0.910 ± 0.085	3.69 ± 0.325
MAIQ	1.50 ± 0.121	2.42 ± 0.197	2.68 ± 0.201
HMIQ	1.20 ± 0.151	0.635 ± 0.042	2.12 ± 0.199
HU	581 ± 20.5	8210 ± 51.0	2840 ± 36.3
GEM	0.526 ± 0.076	46.5 ± 2.01	53.7 ± 1.93

[a] IC50 is the concentration of the compounds producing 50% inhibition of cell growth. Values are the mean ± S.D. of three separate experiments, each performed in duplicate.

Table 2
RR inhibitory potency and subunit-selectivity of the HCTs.

Compound	IC50 ± S.D. (μM)[a]		Average potency[b]	Subunit-selectivity[c]
	M2–M1	p53R2–M1		
3AP	0.385 ± 0.021	0.116 ± 0.007	0.251	3.33
3AP + iron[d]	0.175 ± 0.010	0.115 ± 0.006	0.145	1.52
3MAP	0.202 ± 0.007	0.120 ± 0.005	0.161	1.68
3MAP + iron	0.091 ± 0.005	0.082 ± 0.006	0.087	1.11
DAP	3.54 ± 0.202	0.672 ± 0.047	2.11	5.27
DAP + iron	1.39 ± 0.082	1.10 ± 0.061	1.25	1.27
HMIQ	0.180 ± 0.010	0.012 ± 0.001	0.096	15.0
HMIQ + iron	0.140 ± 0.011	0.171 ± 0.009	0.156	0.819
MAIQ	0.360 ± 0.025	0.075 ± 0.003	0.218	4.80
MAIQ + iron	0.288 ± 0.009	0.275 ± 0.017	0.282	1.05
HU	182 ± 8.52	206 ± 7.50	194	0.883
HU + iron	601 ± 26.3	2120 ± 81.5	1360	0.283

[a] IC50 is the concentration of the compounds producing 50% inhibition of the recombinant RR activity. Values are the mean ± S.D. of three separate experiments, each performed in duplicate.
[b] [IC50 (M2) + IC50 (p53R2)]/2.
[c] IC50 (M2)/IC50 (p53R2).
[d] $FeCl_3$ was added to the reaction mixture.

(data not shown), which was consistent with the results of the cell proliferation assays.

3.2. Inhibitory properties of the HCTs for two forms of RR

Inhibitory properties of the HCTs for two forms of RR (M2–M1 and p53R2–M1) were tested with or without addition of iron in the reaction mixture of the in vitro RR activity assay (Table 2). These compounds were shown to decrease the activities of both recombinant RRs in a dose-dependent manner (Fig. 2). In the absence of iron, the average potency of the HCTs for two RRs was about 100–1000-fold higher than that of HU, and the HCTs inhibited p53R2–M1 more than M2–M1. The addition of iron increased the average potency of the HCTs especially for M2–M1 but decreased their selectivity, resulting in almost no preference for either RR. Among these tested compounds, HMIQ mostly inhibited p53R2–M1 in the absence of iron, while 3MAP showed the highest inhibitory activity and 3AP showed more selectivity for p53R2–M1 in the presence of iron. In contrast, the average potency of HU was similar for M2–M1 and p53R2–M1 in the absence of iron. In the presence of iron, however, the average potency of HU was about 7-fold reduced, resulting in 1000-fold difference in inhibitory activity for the two RRs compared with the HCTs. However, with iron, HU showed significant inhibitory selectivity for M2–M1.

3.3. The HCTs generate reactive oxygen species which quench the diiron-tyrosyl radical center of RR small subunits

We have confirmed that ferrous-3AP complex is the main functional species of this drug and it mediates formation of reactive oxygen species (ROS) that quench the tyrosyl radical of the small subunits and hence inactivate RR [30]. The spin trapping and room temperature EPR measurements showed that 3MAP and DAP also generated the same ROS spectra as 3AP (Fig. 3). EPR measurements on frozen samples of M2 and p53R2 showed that the tyrosyl radical was quenched by ferrous complexes of 3MAP and DAP (Fig. 4). Therefore, probably it is the common mechanism of action for these HCTs that the compounds form ferrous complexes and generate ROS, which inhibit the tyrosyl radical of the small subunits of RRs.

3.4. The HCTs bind to the small subunits of RR

It would be of interest whether these HCTs can directly bind to the RR proteins. Using 3AP as a model, radioligand binding assay was performed to test the binding affinity between the compound and the recombinant RR proteins (Table 3). It was showed that [^{3}H]3AP bound to M2 in a dose-dependent manner. The total binding reaction was substantially inhibited by pre-incubating M2 with a 10-fold molar excess of radioinert 3AP. The nonspecific binding amount of [^{3}H]3AP with BSA was close to that of M2. The radioligand binding reached balance at about 10–20 min. While [^{3}H]3AP bound to M2 and p53R2 similarly, the radioligand almost bound to neither M1 nor the holoenzymes as compared with the nonspecific binding to BSA. Addition of $FeCl_3$ had little effect on the binding. Further addition of the reductant DTT decreased the binding affinity.

4. Discussion

RR catalyzes a key step in the synthesis of dNTPs for DNA replication and damage repair. RR small subunits possess a diiron-

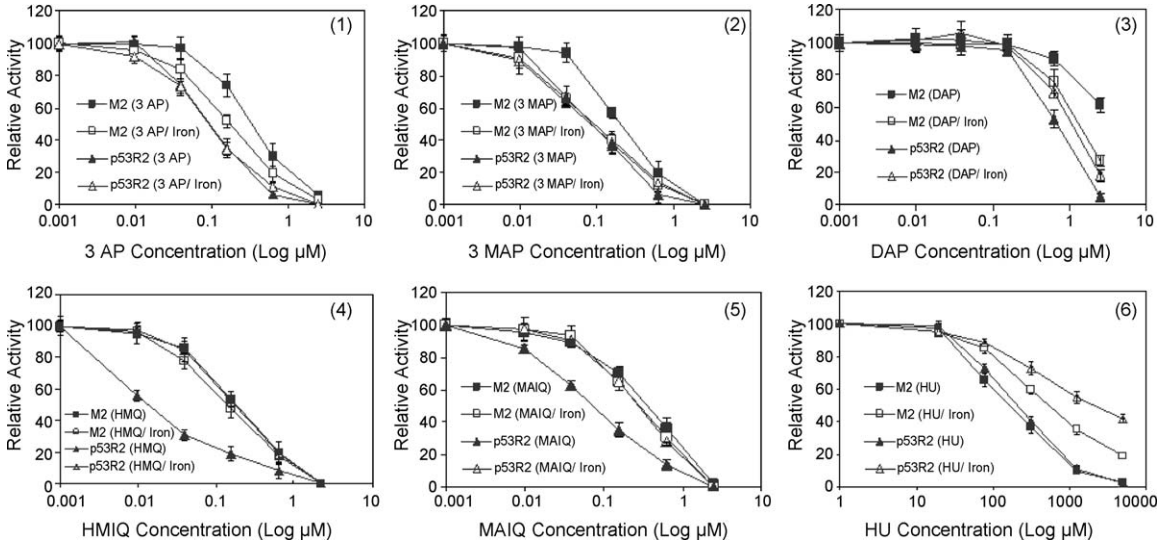

Fig. 2. Inhibitory effects of the HCTs on the activity of two forms of RR. Each of the HCTs was 4-fold serially diluted from 2.50 to 0.010 μM. HU was 4-fold serially diluted from 5000 to 19.5 μM. Various concentrations of each compound were incubated with 0.25 μM RR holoenzyme (M2–M1 or p53R2–M1) followed by the enzymatic activity assay. Where indicated, $FeCl_3$ was added to the reaction mixture. Values are the mean ± S.D. of three separate experiments, each performed at least in duplicate.

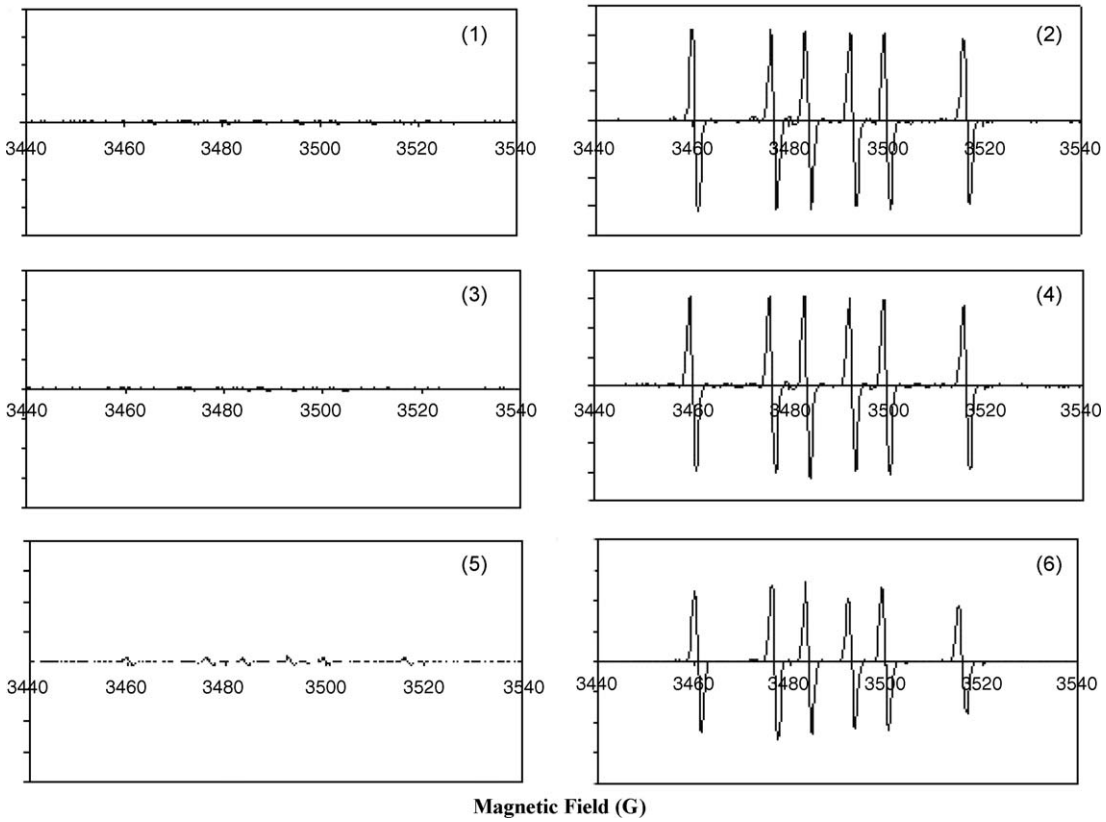

Fig. 3. Room temperature EPR spectra of samples containing DMPO (100 mM), DMSO (5%), and (1) 1 mM 3AP, (2) 1 mM Fe(II)-3AP, (3) 1 mM 3MAP, (4) 1 mM Fe(II)-3MAP, (5) 1 mM DAP, (6) 1 mM Fe(II)-DAP. The solvent was 50 mM HEPES (pH 7.5). Instrumental variables: microwave frequency = 9.798 GHz, microwave power = 0.638 mW, modulation amplitude = 1 G, modulation frequency = 100 KHz.

tyrosyl radical co-factor that is essential for enzyme activity. Destroying the diiron-tyrosyl radical inactivates RR, stops DNA synthesis, and hence inhibits cell proliferation. It is known that HCTs can chelate iron, inhibit RR activity, and thereby inhibit tumor cell growth [25,27,29]. We have previously demonstrated that 3AP, one of the HCTs, targets the diiron-tyrosyl radical [30]. Ferrous-3AP complex is the main functional species of this drug and it mediates formation of ROS that quench the tyrosyl radical of the small subunits and hence inactivate RR. Furthermore, the tyrosyl radicals are not quenched and the enzyme activity is maintained in RR protein samples supplemented with the standard anti-ROS agent catalase, and catalase markedly decreases the antiproliferative effect of 3AP in cytotoxicity assays, thus indicating that the cytotoxicity of 3AP is related with the intracellular generation of ROS and RR inactivation. In the present study, all 8 tested HCTs displayed high potency and close activity against wild-type KB cells and HU- and GEM-resistant KB cells. In vitro RR assays demonstrated that these 3AP analogs inactivated two RRs in a dose-dependent manner, which was parallel with their activity on cell proliferation inhibition. Radioligand binding assays provided direct evidence to confirm that 3AP specifically bound to M2 and p53R2 similarly but not to M1 or the holoenzymes of RR. Spin trapping and EPR measurements showed that like 3AP, the ferrous complexes of 3MAP and DAP mediated ROS generation under aerobic condition, which inhibited the tyrosyl radical of the small subunits. Taken together, the above findings strongly suggest that ROS may be a common mechanism for RR inhibition and at least partially responsible for the antiproliferation activity of these HCTs. Besides, as an intrinsic nature of chelators, they may also chelate the protein-bound iron and affect the tyrosyl radical stability in intact cells. Furthermore, some HCTs can directly cause breakage of tumor cell DNA [15]. Thus, HCTs are not only a potent inhibitor of DNA synthesis and repair through RR inactivation, but also a DNA damaging agent. The dual functions account for their high inhibitory activity and its efficacy against the HU- and GEM-resistant cancer cells (Fig. 5).

In vitro RR assays demonstrated that without the added iron, the HCTs, typically like HMIQ and DAP, showed a selective inhibition for p53R2–M1, while the addition of iron increased the average potency of these compounds especially for M2–M1 but decreased their selectivity for two RRs, such as 3AP and 3MAP. The higher efficiency of the HCTs at inhibiting p53R2–M1 in the absence of added iron is possibly because p53R2 is more susceptible to iron chelators due to a more accessible diiron-tyrosyl radical center in the protein to the environment, as compared with M2 [6]. The diiron-tyrosyl radical center of the small subunits and hence the RR enzymatic activity can be regenerated with iron and the reductant DTT after inhibition, and the regeneration is more significant for p53R2–M1 probably because of the difference in the redox status of M2 and p53P2 [15,37]. Addition of iron promotes the forming of ROS generated by the ferrous complexes of the HCTs and increases the inhibitory potency of the compounds for both RRs, however on the other hand, the different regeneration property of the two small subunits results in a similar sensitivity of two RRs to these compounds.

Both the HCTs and HU inhibit cell growth and RR activity by targeting the diiron-tyrosyl radical co-factor of the small subunits. However, the molecular mechanism and efficacy are different. The HCTs destroy the tyrosyl radical via forming a redox-active complex with iron and generating ROS, which results in radical destruction and RR inactivation. The presence of iron is required for effective enzyme inhibition by the HCTs. HU inactivates RR by directly reducing the diiron-tyrosyl radical co-factor of the small subunits via one-electron transfer from the drug [38,39]. The –NH–

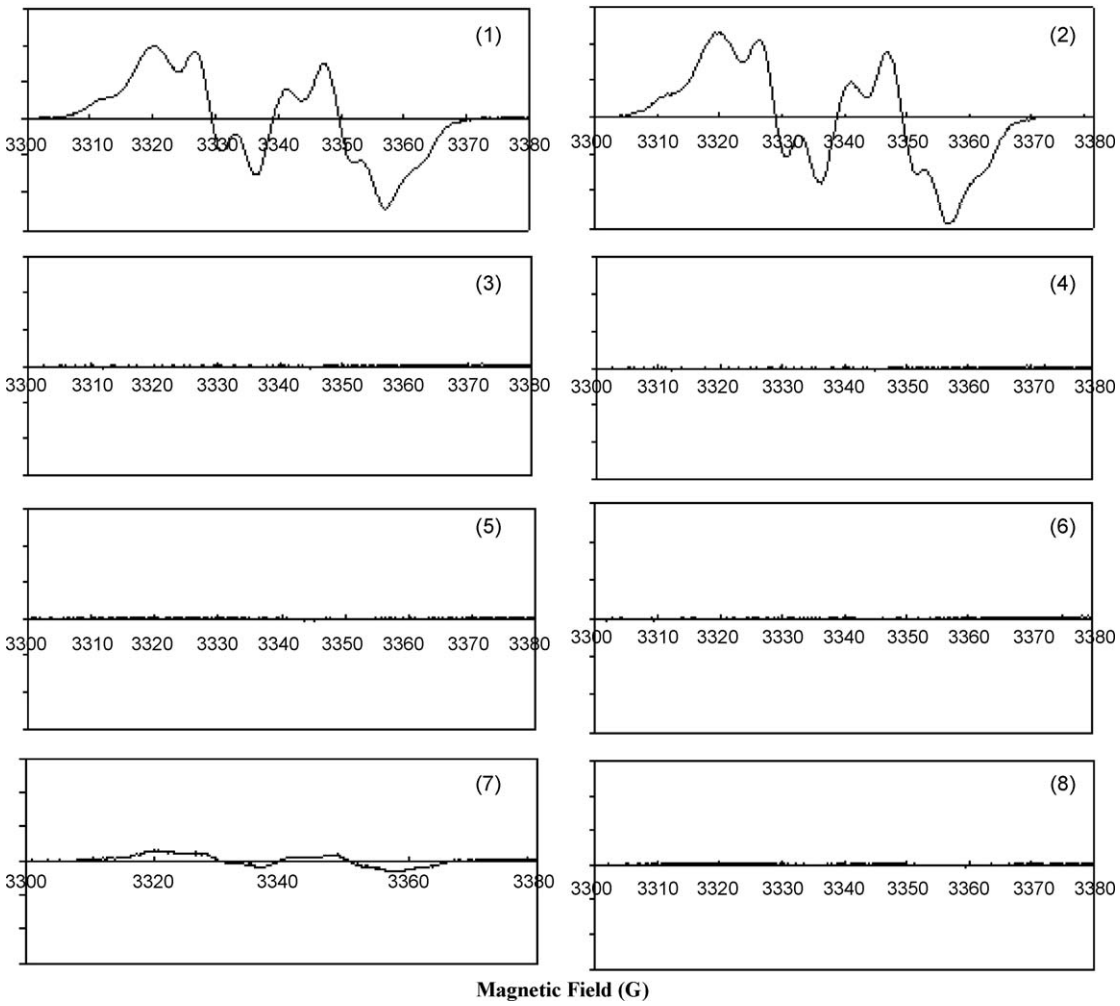

Fig. 4. EPR spectra of frozen samples containing (1) 35 μM M2, (2) 35 μM p53R2, (3) M2 and 5 μM Fe(II)-3AP, (4) p53R2 and 5 μM Fe(II)-3AP, (5) M2 and 5 μM Fe(II)-3MAP, (6) p53R2 and 5 μM Fe(II)-3MAP, (7) M2 and 5 μM Fe(II)-DAP, (8) p53R2 and 5 μM Fe(II)-DAP. Instrumental variables: microwave frequency = 9.376 GHz, microwave power = 0.5 mW, modulation amplitude = 4 G, modulation frequency = 100 KHz, and temperature at sample = 20 K.

Table 3
Binding affinity of [^{3}H]3AP for RR proteins.

[^{3}H]3AP (μm)	Radioligand binding ([^{3}H]3AP (cpm)/M2 (100 pmol))[a]					
	Total binding (M2 + [^{3}H]3AP)	Nonspecific binding (M2 + 3AP + [^{3}H]3AP)		Specific binding (calculated)		Control (BSA + [^{3}H]3AP)
2	400	240		160		360
5	1400	840		560		760
20	4560	1960		2600		2240
50	11600	6800		4800		7600

Time (min)[b]	0	1	5	10	20	40
Total radioligand binding ([^{3}H]3AP (cpm)/M2 (100 pmol))	1920	2040	2480	3200	3360	2280

Proteins	Total radioligand binding ([^{3}H]3AP (cpm)/protein (100 pmol))[c]			
	[^{3}H]3AP	+ $FeCl_3$	+ $FeCl_3$, DTT	+ DTT
M2	3920	4800	1608	1860
p53R2	5040	4360	2400	1560
M1	1320	–	–	–
M2–M1	960	–	–	–
p53R2–M1	680	–	–	–

[a] Total ligand binding values were obtained by incubation of 10 μM M2 with 2, 5, 20, and 50 μM [^{3}H]3AP, respectively. Nonspecific binding was measured by incubation 10 μM M2 with 100 μM radioinert 3AP for 15 min at 37 °C followed by incubation with [^{3}H]3AP for another 15 min at 37 °C. Instead of M2, 10 μM BSA was used as a protein control for evaluation of nonspecific binding. Specific binding = (total binding − nonspecific binding).

[b] Time course for total radioligand binding was determined by incubation of 5 μM M2 with 10 μM [^{3}H]3AP for up to 40 min at 37 °C.

[c] Comparison of the binding affinity of RR subunits and holoenzymes to [^{3}H]3AP was performed by incubation of 5 μM RR subunit or holoenzyme protein with 10 μM [^{3}H]3AP for 15 min at 37 °C, where indicated 50 μM $FeCl_3$ and/or 500 μM DTT were added. RR holoenzymes were made by incubation of M1 with M2, or M1 with p53R2 for 10 min at 37 °C before adding [^{3}H]3AP. Values are the mean of duplicates.

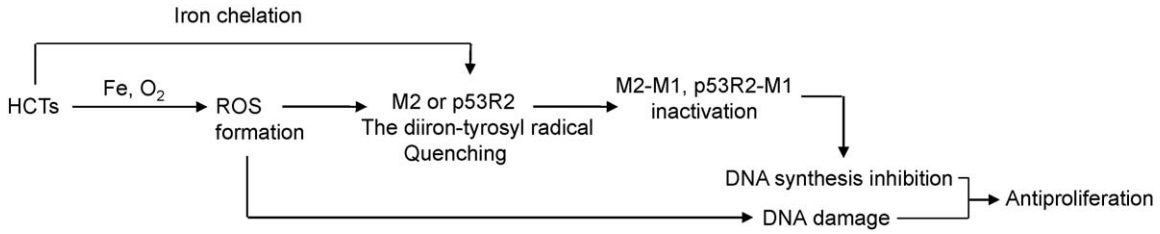

Fig. 5. Scheme for the inhibitory mechanisms of HCTs for two forms of RR.

OH segment of HU is the minimal structural requirement for its inhibitory activity [31]. In the absence of iron, HU inhibited both small subunits at a similar level. However, the inhibition was reversed significantly in the presence of iron and DTT. The regeneration was much more marked for p53R2 resulting in a selective inhibition of M2 more than p53R2. Since cells have both, an iron pool and reductants, possibly the HCTs almost equally inhibit two forms of RR while HU possesses inhibitory selectivity for M2/M1 in vivo [31].

The clinical use of RR inhibitors has several decades of history, which has demonstrated that RR inhibitors have anti-tumor activity both as a single agent and as enhancers of other anticancer drugs. However, 3AP-related adverse events have been observed including methemoglobinemia and hypoxia, which could cause acute symptoms in patients with limited pulmonary or cardiovascular reserve [40]. The drug-induced ROS may oxidize ferrous hemoglobin interfering with its oxygen binding and delivery [30]. The drug efficiency of HU is relatively low, which is associated with its physicochemical properties, e.g., very high hydrophilicity and small molecular size. Often induced resistance to HU in cancer cells is another shortcoming of the drug [15]. The RR inhibition by the HCTs and HU is partially reversible because of the regeneration in the presence of iron and reductants. Therefore, development of novel small subunit inhibitors that target the diiron-tyrosyl radical co-factor, but with new inhibitory mechanisms is a challenge for future generations of anticancer drugs.

M2 and p53R2 play different roles in DNA replication and damage repair, respectively. Development of subunit-specific inhibitors for different clinical applications is an attractive direction. Upon DNA damage, cancer cells often cannot induce p53R2 due to the lack of p53, whereas normal cells can repair their DNA with help from induced p53R2. Thus, use of DNA-damaging chemotherapeutic agents in combination with specific inhibitors of M2 is a potential therapeutic strategy to selectively kill cancer cells, especially those with overexpressed M2. On the other hand, inhibitors specific for p53R2 may be useful for targeting tumors that overexpress p53R2, because its inhibition increases the sensitivity of cells to DNA damaging agents [9,21,22,41]. The high potency of the HCTs makes them a reasonable starting point for rational design of more potent and subunit-selective RR inhibitors for cancer therapy.

Acknowledgements

This research was supported by grants from the National Natural Science Foundation of China (30873094), Zhejiang Provincial Science and Technology Research Program (2008C23070), and the Scientific Research Foundation for the Returned Overseas Chinese Scholars, State Education Ministry (2008-101).

References

[1] Nordlund P, Reichard P. Ribonucleotide reductases. Annu Rev Biochem 2006; 75:681–706.
[2] Tanaka H, Arakawa H, Yamaguchi T, Shiraishi K, Fukuda S, Matsui K, et al. A ribonucleotide reductase gene involved in a p53-dependent cell-cycle checkpoint for DNA damage. Nature 2000;404:42–9.
[3] Nakano K, Balint E, Ashcroft M, Vousden KH. A ribonucleotide reductase gene is a transcriptional target of p53 and p73. Oncogene 2000;19:4283–9.
[4] Guittet O, Hakansson P, Voevodskaya N, Fridd S, Graslund A, Arakawa H, et al. Mammalian p53R2 protein forms an active ribonucleotide reductase in vitro with the R1 protein, which is expressed both in resting cells in response to DNA damage and in proliferating cells. J Biol Chem 2001;276:40647–51.
[5] Chabes AL, Bjorklund S, Thelander L. S Phase-specific transcription of the mouse ribonucleotide reductase R2 gene requires both a proximal repressive E2F-binding site and an upstream promoter activating region. J Biol Chem 2004;279: 10796–807.
[6] Shao J, Zhou B, Zhu L, Qiu W, Yuan YC, Xi B, et al. In vitro characterization of enzymatic properties and inhibition of the p53R2 subunit of human ribonucleotide reductase. Cancer Res 2004;64:1–6.
[7] Xue L, Zhou B, Liu X, Qiu W, Jin Z, Yen Y. Wild-type p53 regulates human ribonucleotide reductase by protein–protein interaction with p53R2 as well as hRRM2 subunits. Cancer Res 2003;63:980–6.
[8] Chang L, Zhou B, Hu S, Guo R, Liu X, Jones SN, et al. ATM-mediated serine 72 phosphorylation stabilizes ribonucleotide reductase small subunit p53R2 protein against MDM2 to DNA damage. Proc Natl Acad Sci USA 2008;105: 18519–24.
[9] Lozano G, Elledge SJ. p53 sends nucleotides to repair DNA. Nature 2000;404: 24–5.
[10] Kimura T, Takeda S, Sagiya Y, Gotoh M, Nakamura Y, Arakawa H. Impaired function of p53R2 in Rrm2b-null mice causes severe renal failure through attenuation of dNTP pools. Nat Genet 2003;34:440–5.
[11] Thelander L. Ribonucleotide reductase and mitochondrial DNA synthesis. Nat Genet 2007;39:703–4.
[12] Pontarin G, Ferraro P, Hakansson P, Thelander L, Reichard P, Bianchi V. p53R2-dependent ribonucleotide reduction provides deoxyribonucleotides in quiescent human fibroblasts in the absence of induced DNA damage. J Biol Chem 2007;282:16820–8.
[13] Bourdon A, Minai L, Serre V, Jais JP, Sarzi E, Aubert S, et al. Mutation of RRM2B, encoding p53-controlled ribonucleotide reductase (p53R2), causes severe mitochondrial DNA depletion. Nat Genet 2007;39:776–80.
[14] Kollberg G, Darin N, Benan K, Moslemi AR, Lindal S, Tulinius M, et al. A novel homozygous RRM2B missense mutation in association with severe mtDNA depletion. Neuromuscul Disord 2009;19:147–50.
[15] Shao J, Zhou B, Chu B, Yen Y. Ribonucleotide reductase inhibitors and future drug design. Curr Cancer Drug Targets 2006;6:409–31.
[16] Zhang K, Hu S, Wu J, Chen L, Lu J, Wang X, et al. Overexpression of RRM2 decreases thrombspondin-1 and increases VEGF production in human cancer cells in vitro and in vivo: implication of RRM2 in angiogenesis. Mol Cancer 2009;8:11.
[17] Giles FJ. A new era for ribonucleoside reductase inhibition. Leuk Res 2007; 31:1171–2.
[18] Okumura H, Natsugoe S, Yokomakura N, Kita Y, Matsumoto M, Uchikado Y, et al. Expression of p53R2 is related to prognosis in patients with esophageal squamous cell carcinoma. Clin Cancer Res 2006;12:3740–5.
[19] Yanamoto S, Kawasaki G, Yamada SI, Yoshitomi I, Yoshida H, Mizuno A. Ribonucleotide reductase small subunit p53R2 promotes oral cancer invasion via the E-cadherin/beta-catenin pathway. Oral Oncol 2008 [Epub ahead of print].
[20] Liu X, Zhou B, Xue L, Yen F, Chu P, Un F, et al. Ribonucleotide reductase subunits M2 and p53R2 are potential biomarkers for metastasis of colon cancer. Clin Colorectal Cancer 2007;6:374–81.
[21] Devlin HL, Mack PC, Burich RA, Gumerlock PH, Kung HJ, Mudryj M, et al. Impairment of the DNA repair and growth arrest pathways by p53R2 silencing enhances DNA damage-induced apoptosis in a p53-dependent manner in prostate cancer cells. Mol Cancer Res 2008;6:808–18.
[22] Wang X, Zhenchuk A, Wiman KG, Albertioni F. Regulation of p53R2 and its role as potential target for cancer therapy. Cancer Lett 2009;276:1–7.
[23] Kim SO, Jeong JY, Kim MR, Cho HJ, Ju JY, Kwon YS, et al. Efficacy of gemcitabine in patients with non-small cell lung cancer according to promoter polymorphisms of the ribonucleotide reductase M1 gene. Clin Cancer Res 2008;14:3083–8.
[24] Saban N, Bujak M. Hydroxyurea and hydroxamic acid derivatives as antitumor drugs. Cancer Chemother Pharmacol)2009;(April (7)) [Epub ahead of print].
[25] Finch RA, Liu M, Grill SP, Rose WC, Loomis R, Vasquez KM, et al. Triapine (3-aminopyridine-2-carboxaldehyde-thiosemicarbazone): a potent inhibitor of

ribonucleotide reductase activity with broad spectrum antitumor activity. Biochem Pharmacol 2000;59:983–91.
[26] Xu H, Fairman JW, Wijerathna SR, Kreischer NR, LaMacchia J, Helmbrecht E, et al. The structural basis for peptidomimetic inhibition of eukaryotic ribonucleotide reductase: a conformationally flexible pharmacophore. J Med Chem 2008;51: 4653–9.
[27] Cory JG, Cory AH, Rappa G, Lorico A, Liu MC, Lin TS, et al. Structure–function relationships for a new series of pyridine-2-carboxaldehyde thiosemicarbazones on ribonucleotide reductase activity and tumor cell growth in culture and in vivo. Adv Enzyme Regul 1995;35:55–68.
[28] Gojo I, Tidwell ML, Greer J, Takebe N, Seiter K, Pochron MF, et al. Phase I and pharmacokinetic study of Triapine((R)), a potent ribonucleotide reductase inhibitor, in adults with advanced hematologic malignancies. Leuk Res 2007;31:1173–81.
[29] Chaston TB, Lovejoy DB, Watts RN, Richardson DR. Examination of the antiproliferative activity of iron chelators: multiple cellular targets and the different mechanism of action of triapine compared with desferrioxamine and the potent pyridoxal isonicotinoyl hydrazone analogue 311. Clin Cancer Res 2003;9:402–14.
[30] Shao J, Zhou B, Di Bilio AJ, Zhu L, Wang T, Qi C, et al. A ferrous–triapine complex mediates formation of reactive oxygen species that inactivate human ribonucleotide reductase. Mol Cancer Ther 2006;5:586–92.
[31] Shao J, Zhou B, Zhu L, Bilio AJ, Su L, Yuan YC, et al. Determination of the potency and subunit-selectivity of ribonucleotide reductase inhibitors with a recombinant-holoenzyme-based in vitro assay. Biochem Pharmacol 2005;69:627–34.
[32] Yen Y, Grill SP, Dutschman GE, Chang CN, Zhou BS, Cheng YC. Characterization of a hydroxyurea-resistant human KB cell line with supersensitivity to 6-thioguanine. Cancer Res 1994;54:3686–91.
[33] Goan YG, Zhou B, Hu E, Mi S, Yen Y. Overexpression of ribonucleotide reductase as a mechanism of resistance to 2,2-difluorodeoxycitidine in the human KB cancer cell line. Cancer Res 1999;59:4204–7.
[34] Heidel JD, Liu JY, Yen Y, Zhou B, Heale BS, Rossi JJ, et al. Potent siRNA inhibitors of ribonucleotide reductase subunit RRM2 reduce cell proliferation in vitro and in vivo. Clin Cancer Res 2007;13:2207–15.
[35] Solly K, Wang X, Xu X, Strulovici B, Zheng W. Application of real-time cell electronic sensing (RT-CES) technology to cell-based assays. Assay Drug Dev Technol 2004;2:363–72.
[36] Tarpey MM, Wink DA, Grisham MB. Methods for detection of reactive metabolites of oxygen and nitrogen: in vitro and in vivo considerations. Am J Physiol Regul Integr Comp Physiol 2004;286:R431–444.
[37] Liu X, Xue L, Yen Y. Redox property of ribonucleotide reductase small subunit M2 and p53R2. Methods Mol Biol 2008;477:195–206.
[38] Lassmann G, Thelander L, Gräslund A. EPR stopped-flow studies of the reaction of the tyrosyl radical of protein R2 from ribonucleotide reductase with hydroxyurea. Biochem Biophys Res Commun 1992;188:879–87.
[39] Nyholm S, Thelander L, Graslund A. Reduction and loss of the iron center in the reaction of the small subunit of mouse ribonucleotide reductase with hydroxyurea. Biochemistry 1993;32:11569–74.
[40] Yen Y, Margolin K, Doroshow J, Fishman M, Johnson B, Clairmont C, et al. A phase I trial of 3-aminopyridine-2-carboxaldehyde thiosemicarbazone in combination with gemcitabine for patients with advanced cancer. Cancer Chemother Pharmacol 2004;54:331–42.
[41] Lin ZP, Belcourt MF, Cory JG, Sartorelli AC. Stable suppression of the R2 subunit of ribonucleotide reductase by R2-targeted siRNA sensitizes p53 (−/−) HCT-116 colon cancer cells to DNA-damaging agents and ribonucleotide reductase inhibitors. J Biol Chem 2004;279:27030–8.